Cell Biology:

Functional Swapping between Transmembrane Protein TMEM16A and TMEM16F

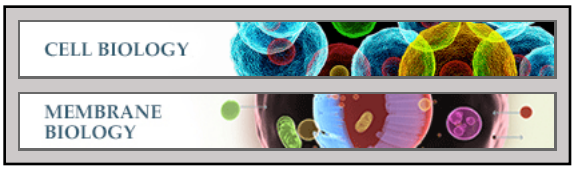

Takayuki Suzuki, Jun Suzuki and Shigekazu Nagata

J. Biol. Chem. *published online January 28, 2014*

Access the most updated version of this article at doi: 10.1074/jbc.M113.542324

Supplemental material:
http://www.jbc.org/content/suppl/2014/01/28/M113.542324.DC1.html

This article cites 0 references, 0 of which can be accessed free at
http://www.jbc.org/content/early/2014/01/28/jbc.M113.542324.full.html#ref-list-1

JBC Papers in Press. Published on January 28, 2014 as Manuscript M113.542324
The latest version is at http://www.jbc.org/cgi/doi/10.1074/jbc.M113.542324

Functional Swapping between Transmembrane Protein TMEM16A and TMEM16F*

Takayuki Suzuki[1], Jun Suzuki[1] and Shigekazu Nagata[1,2]

[1]*From the Department of Medical Chemistry, Graduate School of Medicine, Kyoto University, Yoshida, Sakyo-ku, Kyoto 606-8501, Japan*

[2]*Core Research for Evolutional Science and Technology, Japan Science and Technology Corporation, Kyoto 606-8501, Japan*

*Running title: Functional swapping between TMEM16A and TMEM16F

To whom Correspondence should be addressed: Shigekazu Nagata, Department of Medical Chemistry, Graduate School of Medicine, Kyoto University, Yoshida, Sakyo-ku, Kyoto 606-8501, Japan, Tel.: 81-75-753-9441; Fax: 81-75-753-9446; E-mail: snagata@mfour.med.kyoto-u.ac.jp

Keywords: phospholipid scramblase; Cl^- channel; deletion mutation; swapping; chemical inhibitors

Background: TMEM16A and 16F function as a Ca^{2+}-dependent Cl^- channel and phospholipid-scramblase, respectively.

Results: The N- and C-terminal domains of TMEM16A and 16F are exchangeable, and are necessary for ER exit and stability.

Conclusion: TMEM16A and 16F use a similar mechanism for transporting and stabilizing protein, but their functional domains differ.

Significance: Identifying functional domains will lead to better understanding of TMEM16 family.

SUMMARY

The transmembrane proteins TMEM16A and 16F each carry eight transmembrane regions with cytoplasmic N- and C-termini. TMEM16A carries out Ca^{2+}-dependent Cl^- ion transport, and TMEM16F is responsible for Ca^{2+}-dependent phospholipid scrambling. We here established an assay system for the Ca^{2+}-dependent Cl^- channel activity using 293T cells, and for the phospholipid scramblase activity using *TMEM16F*$^{-/-}$ immortalized fetal thymocytes (IFETs). Chemical cross-linking analysis showed that TMEM16A and 16F form homodimers in both 293T cells and IFETs. Successive deletion from the N- or C-terminus of both proteins and the swapping of regions between TMEM16A and 16F indicated that their cytoplasmic N-terminal (147 amino acids for TMEM16A and 95 for 16F), and C-terminal (88 amino acids for TMEM16A and 68 for 16F) regions were essential for their localization at plasma membranes and protein stability, respectively, and could be exchanged. Analyses of TMEM16A and 16F mutants with point mutations in the pore region (located

between the 5th and 6th transmembrane regions) indicated that the pore region is essential for both 16A's Cl^- channel activity and 16F's phospholipid scramblase activity. Some chemicals such as epigallocatechin-3-gallate and digallic acid inhibited TMEM16A's Cl^- channel activity and 16F's scramblase activity with an opposite preference. These results indicate that TMEM16A and 16F use a similar mechanism for sorting to plasma membrane and protein stabilization, but their functional domains significantly differ.

The transmembrane protein (TMEM)16, also called Anoctamin (Ano), family members carry 8 transmembrane domains and have cytoplasmic N- and C-termini (1,2). This family consists of 10 members that have 20-60 % amino acid-sequence identity. TMEM16A (Ano1) and 16B (Ano2) have a Ca^{2+}-dependent Cl^- channel activity (3-5) that mediates various biological processes, including transepithelial secretion, sensory transduction, and smooth muscle contraction (6). TMEM16A is expressed ubiquitously, while TMEM16B is expressed in a limited set of tissues, such as the brain and eyes (7,8).

The functions of other TMEM16 family members have been elusive, but we found that TMEM16F (Ano6) as well as 16C (Ano3), 16D (Ano4), 16G (Ano7), and 16J (Ano9) are involved in Ca^{2+}-dependent phospholipid scrambling (9,10). In particular, we and others showed that TMEM16F is ubiquitously expressed in various cells, including hematopoietic cells, and is involved in the phosphatidylserine (PS) exposure on activated platelets required for blood clotting (9,11,12). TMEM16F is expressed in osteoblasts, and was recently shown to be involved in mineralized bone matrix production during skeletal development (13). In addition, abnormalities (mutations and over-expression) in TMEM16 family members are implicated in a number of human diseases (6). For example, genetic mutations in TMEM16C, 16E, 16F, and 16K are, respectively, associated with craniocervical dystonia (14), musculoskeletal disorder (15,16), bleeding disorder (9), and cerebellar ataxia (17). TMEM16A is overexpressed in human gastrointestinal stromal tumors and in head and neck squamous carcinoma; TMEM16G is overexpressed in prostate cancer (18,19). Thus, compounds that modulate TMEM16A's function have been explored for the treatment of human diseases such as cystic fibrosis, hypertension, secretory diarrheas, asthma, and cancer (20). However, despite the apparently important physiological and pathological roles of TMEM16 family members, very little is known about the molecular mechanisms by which they exert their Cl^- channel or phospholipid scramblase functions.

In this report, we prepared a series of N- and C-terminal deletion mutants for TMEM16A and 16F, and showed that these regions are essential for their localization at plasma membrane and protein stability, respectively. These essential regions, which comprise about one third of the molecule, were exchangeable between TMEM16A and 16F. Point mutations in the "pore" domain in TMEM16F indicated that this domain is important for the protein's scramblase activity, as is true for TMEM16A's Cl^- channel

activity. In addition, we found some chemicals preferentially inhibit TMEM16A's Cl^- channel activity, while others preferentially inhibit 16F's scramblase activity. These results indicate that TMEM16A and 16F use a similar mechanism to stabilize and localize them at plasma membranes, but their functional domains are significantly different.

EXPERIMENTAL PROCEDURES

Chemicals and Cell Lines---Tannic acid and epigallocatechin-3-gallate (EGCG) were purchased from Nacalai. Digallic acid and aminophenylthiazole $T16A_{inh}$-A01 (2-(5-ethyl-4-hydroxy-6-methylpyrimidin-2-ylthio)-N-(4-(4-methoxyphenyl) thiazol-2-yl)acetamide) were from Santa Cruz, and Millipore, respectively. NPPB (5-nitro-2-(3-phenylpropylamino)benzoic acid), DIDS (4,4'-diisothiocyanostilbene-2,2'- disulfonic acid), and 2-[3-(trifluoromethyl)anilino] nicotinic acid (niflumic acid) were purchased from Sigma. The crosslinker dithiobis[succinimidylpropionate] (DSP) was purchased from Thermo Scientific.

Mouse *TMEM16F*$^{-/-}$ immortalized fetal thymocytes (IFETs) were described previously (10), and maintained in RPMI 1640 medium (Gibco) supplemented with 10% fetal calf serum (FCS, Gibco) and 50 μM β-mercaptoethanol. Human HEK293T and Plat-E cells (21) were cultured in DMEM (Gibco) containing 10% FCS.

Expression Plasmids for Mouse TMEM16A and 16F cDNAs, and Their Mutants---Mouse TMEM16F cDNA (GenBank: NM_175344) was described previously (9). The full-length cDNA for mouse TMEM16A (GenBank: BC062959.1) was purchased from DNAFORM. The cDNAs for the TMEM16A and TMEM16F mutants, and their chimeric molecules were prepared by recombinant PCR with the full-length TMEM16A and TMEM16F cDNAs as templates. The authenticity of the respective cDNAs was verified by sequencing.

Transformation of TMEM16F$^{-/-}$ *IFETs*---The full-length cDNA for TMEM16A, TMEM16F, or their mutants was inserted at *Eco* RI or between the *Bam* HI and *Eco* RI sites of the mouse retroviral vector pMXs puro c-Flag to express a protein that was Flag-tagged at the C-terminus (9). Retroviruses were produced in Plat-E cells, concentrated by centrifugation at 6,000 × *g* for 16 h at 4°C, and used to infect *TMEM16F*$^{-/-}$ IFETs as described previously (10). Transformants were selected by culturing the cells in the presence of 1 μg/ml puromycin.

Analysis of Phosphatidylserine-Exposure---The Ca^{2+}-induced PS exposure was analyzed essentially as previously described (9). In brief, 5×10^5 IFETs were suspended in 1 ml of 10 mM HEPES-NaOH buffer (pH 7.5) containing 140 mM NaCl, 2.5 mM $CaCl_2$, 5 μg/ml propidium iodide (PI), and 1000-fold diluted Cy5-labeled AnnexinV (BioVision). The cells were treated at room temperature with 3 μM A23187 (Sigma), followed by flow cytometry using a FACSCalibur (BD Bioscience). PI-positive cells were excluded from the analysis.*Electrophysiology*---The wild-type and mutant TMEM16A and 16F were tagged with Flag at the C-terminus, and introduced into the *Bam* HI or *Eco* RI/*Sal* I sites of pEF-BOS-EX (22). HEK293T cells (2.5×10^5 cells) were

co-transfected with 1 μg of the expression vector and 0.1 μg of pMAX-GFP (Amaxa) by lipofection using FuGENE6 (Promega). Twenty-four hours later, the cells were re-seeded on glass coverslips, and whole-cell patch-clamp recording was performed within 24 h after re-seeding, essentially as previously described (4,23). That is, the cells expressing GFP were voltage-clamped for 500 ms-intervals between -120 mV and +120 mV with 10-mV increments. The holding potential was maintained at 0 mV. Data were acquired using an EPC 8 patch-clamp amplifier (HEKA) and Axograph 4.8 software (Axon Instruments). All experiments were conducted at room temperature. The extracellular solution contained 140 mM NaCl, 5 mM KCl, 2 mM $CaCl_2$, 1 mM $MgCl_2$, 30 mM Glucose, and 10 mM HEPES-NaOH (pH 7.5). The electrodes were filled with a solution containing 140 mM NaCl, 1.12 mM EGTA, 1 mM $CaCl_2$, 30 mM Glucose, and 10 mM HEPES-NaOH (pH 7.5). The free Ca^{2+} concentration (500 nM) was calculated with WEBMAXC software (4).

Western Blotting---Cells were lysed in RIPA buffer [50 mM Tris-HCl buffer (pH 8.0) containing 1% NP-40, 0.1% SDS, 0.5% sodium deoxycholate, 150 mM NaCl] supplemented with a protease inhibitor cocktail (cOmplete Mini, Roche). The lysates were centrifuged at 17,700 × *g* for 15 min at 4 °C, and the supernatants were mixed with 5 × SDS sample buffer [200 mM Tris-HCl (pH 6.8), 10% SDS, 25% glycerol, 5% β-mercaptoethanol, and 0.05% bromophenol blue]. Following incubation for 30 min at room temperature, the samples were separated by PAGE and transferred to a PVDF membrane (Millipore). The proteins were probed with the mouse anti-Flag M2-HRP mAb (Sigma) or mouse anti-α-tubulin mAb (Calbiochem) followed by HRP-conjugated goat anti-mouse Ig Ab (DAKO), and visualized using the Western Lightning Plus-ECL system (PerkinElmer).

Chemical Cross-Linking---HEK293T cells were transfected with the expression vector for Flag-tagged TMEM16A or TMEM16F. Forty-eight hours after transfection, HEK293T cells (2 x 10^6 cells), or *TMEM16F*$^{-/-}$ IFET transformants (2 x 10^6 cells) expressing TMEM16A or TMEM16F were suspended in 1 ml of PBS (Gibco), and incubated with DSP for 30 min at room temperature. The reaction was stopped by adding 20 μl of 1 M glycine (pH 9.2) and incubating for 30 min on ice. After centrifugation, the cells were lysed with RIPA buffer and analyzed by western blotting using SDS-sample buffer without β-mercaptoethanol.

Confocal Fluorescence Microscopy---The wild-type and mutants of TMEM16A and 16F, tagged with GFP at the C-terminus, were introduced into pEF-BOS-EX vector. HEK293T cells (2.5 x 10^5 cells) were transfected with 1 μg of the expression vector by lipofection using FuGENE6. Twenty-four hours later, the cells were re-seeded on glass bottom dish, cultured for 24 h, and observed by confocal microscope (FV1000-D; Olympus).

RESULTS

TMEM16A and TMEM16F---Mouse TMEM16A consists of 956 amino acids, and 16F has 911 amino

acids; both carry eight transmembrane regions and have cytoplasmic N- and C-termini (Fig. S1). Their amino acid sequences are homologous throughout the molecule with an overall identity of 35.4% and similarity of 52.1%, and the regions around the first, fourth to fifth, and sixth to seventh transmembrane regions (amino acids 312 to 356, 576 to 641, and 698 to 787 on 16A) are well conserved (Fig. S1) (71.1, 63.6, and 67.7% identity, respectively).

We assayed the Cl^- channel activity by patch-clamp analysis with human 293T cells that had been transfected with a TMEM16 expression vector (10). To assay the Ca^{2+}-dependent phospholipid scramblase activity, we determined the A23187 Ca^{2+} ionophore-induced PS exposure in *TMEM16F*$^{-/-}$ IFET transformants expressing TMEM16 family members (10). As shown in Figs. 1A and 1B, TMEM16A and 16F were expressed with a similar efficiency in both 293T cells and IFETs. However, 293T cells expressing TMEM16A but not 16F showed Cl^- channel activity, and the A23187-induced PS-exposing activity was observed in TMEM16F-expressing but not 16A-expressing *TMEM16F*$^{-/-}$ IFET transformants. These observations confirmed that TMEM16A has Ca^{2+}-dependent Cl^- channel activity, while 16F functions as a Ca^{2+}-dependent phospholipid scramblase.

Dimerization of TMEM16A and 16F---Sheridan *et al.* (24) previously reported that mouse TMEM16A expressed in 293T cells forms a dimer under non-denaturing conditions. When the cell lysates of 293T cells that had been transfected by a Flag-tagged TMEM16A expression vector were analyzed by SDS-PAGE without a reducing agent, about a half the molecules appeared as dimers with an apparent molecular mass of about 250 kDa (Fig. 2A). Treatment of the transfected 293T cells with the cross-linker DSP dose-dependently increased the percentage of dimers without increasing higher-order complexes, confirming that most of the TMEM16A in transfected 293T cells is present as a dimer. Overexpressed TMEM16A similarly formed dimers in *TMEM16F*$^{-/-}$ IFET transformants. On the other hand, when Flag-tagged TMEM16F expressed in 293T cells or IFETs was analyzed by SDS-PAGE, the protein was found as a monomer with molecular mass of about 100 kDa (Fig. 2B). However, like TMEM16A, when the transfected 293T cells were treated with DSP, TMEM16F appeared as a dimer, and most of the TMEM16F protein was found as a dimer after treatment with 50 μM DSP. Treatment of the IFET transformants expressing Flag-tagged TMEM16F with DSP also revealed TMEM16 dimerization, but not higher-order complex formation. The *TMEM16F*$^{-/-}$ IFETs express TMEM16H and 16K (10), but the mRNA level of the endogenous 16H and 16K is less than 2% of that of the exogenously-introduced TMEM16A or 16F, judged by real-time PCR (data not shown), indicating that TMEM16A and 16F form homodimers.

Successive Deletion from the N- or C-terminus---Mutations or alternative splicings in the cytoplasmic N-terminal tail have a strong effect on the function of TMEM16A and 16F (9,25), suggesting that this region is important for their function. To systematically analyze the contribution of the N- and

C-terminal regions of TMEM16A and 16F, successive deletion mutants were prepared. Since exons are known to code for functional units (26), the mutants were prepared by successively deleting exons from the N- or C-terminus. As shown in Figs. 3A and 3B, deletion of the first exon of TMEM16A had no effect on its Cl^- channel activity. However, the mutant carrying the deletion of its 2^{nd} exon, which corresponds to exons 2, 3, and 4 of 16F, did not show Cl^- channel activity . Similarly, deletion of exons 1 and 2 had no effect on the scramblase activity of TMEM16F, but the mutant with further deletion did not show its scramblase activity (Figs. 3E and 3F). The expressed protein level of Δ1-2 of TMEM16A and Δ1-3 of TMEM16F was reduced compared with the wild-type (Figs. 3C and 3G), but more dramatic change was observed for their cellular localization. That is, the wild-type as well as the functional mutants (Δ1 mutant of TMEM16A and Δ1-2 mutant of TMEM16F) were localized at plasma membranes, while non-functional mutants (Δ1-2 of TMEM16A and Δ1-3 of TMEM16F) were found in the cytoplasm (Figs. 3D and 3H). These results suggested that the inability of these deletion mutants to show the Cl^- channel or scramblase activity was partly because they could not be localized at plasma membrane.

C-terminal deletion mutants for TMEM16A and 16F were similarly prepared, and deletion of the last exon (exon 24 of TMEM16A; exon 20 of TMEM16F) completely abrogated protein expression in both cases (Fig. 4). The mRNA for the exon 24-deleted TMEM16F was present at a similar level as that for the wild-type TMEM16F (data not shown), suggesting that the drastic loss of C-terminal-deleted TMEM16A and 16F protein expression was owing to the extreme instability of the mutant proteins.

Functional Swapping between TMEM16A and 16F at the N- and C-terminus---TMEM16A and 16F perform different functions, Cl^- channel activity and phospholipid scrambling activity, yet the deletion of N-terminal and C-terminal regions had the similar effects on them. To analyze the exchangeability of these regions between TMEM16A and 16F, their exons were swapped at the corresponding regions (Figs. 5A and 6A). For protein expression, the cytoplasmic N-terminal and C-terminal tails were fully exchangeable. That is, the protein level of the chimeric molecules carrying 16F's N- or C-terminal sequence in the nFA or AFc series chimera, or 16A's N- or C-terminal sequence in the nAF or FAc series chimera was similar to or better than that of authentic TMEM16A or 16F (Figs. 5B and 6B). Most of the N-terminal cytoplasmic tail (amino acids 1-285 of 16A and 1-250 of 16F) was also functionally exchangeable. That is, the nFA3 chimera carrying 16F's N-terminal tail was fully active for the Cl^- channel activity (Fig. 5C), and the PS-exposing activity of the nAF3 chimera carrying 16A's N-terminal tail was about 70% of that of the authentic TMEM16F (Fig. 5D). Notably, the nAF1 and nAF2 chimeras, in which the 16A-derived region was shorter than that of nAF3, did not show the PS-scrambling activity. Analyses of cellular localization with GFP-tagged proteins indicated that nAF3, but not nAF1 and nAF2 chimeras, was localized at plasma membrane (Fig. 5E).

The functional exchangeability was observed at C-terminus as well (amino acids 869-956 of TMEM16A and 844-911 of 16F). The AFc1 chimera carrying 16F's C-terminal cytoplasmic tail and the FAc1 chimera carrying 16A's C-terminal cytoplasmic tail worked as Cl^- channel and phosholipid scramblase, respectively (Figs. 6C and 6D). It is notable that the AFc2 chimera carrying a longer 16F-derived C-terminal region (809-911 of 16F) had Cl^- channel activity, while the FAc 2 chimera carrying the corresponding 16A-derived C-terminal region (834-956 of 16A) failed to show the phospholipid scramblase activity (Figs. 6C and 6D)

Point Mutations in the Pore Region---A region called the "pore" is present between the 5th and 6th transmembrane regions of TMEM16A (1), and point mutations in this region affect TMEM16A's ion permeability (5). This pore region (the entire region between the 5th and 6th transmembrane regions) is well conserved between TMEM16A and 16F, with 44.3% identity in the amino acid sequence (Fig. 7A). To examine whether similar amino acids are involved in the Cl^- channel activity of TMEM16A and the phospholipid scramblase activity of TMEM16F, point mutations were introduced into TMEM16A and TMEM16F at three positions (amino acid positions 617, 641, and 664 in TMEM16A, and 592, 616, and 638 in TMEM16F). As shown in Fig. 7C, the replacement of arginine-617 and lysine-641 by glutamic acid in TMEM16A severely inactivated its Cl^- channel activity, while the mutation of lysine 664 by glutamic acid had no effect. Similarly, replacing arginine-592 and lysine-616, but not lysine-638 with glutamic acid significantly inactivated 16F's scramblase activity (Fig. 7D), and replacing both argine-592 and lysine-616 almost completely destroyed its activity. These results suggest that, analogous to its function in TMEM16A, the pore region of TMEM16F plays an important role in its phospholipid scrambling activity.

Effect of Chemical Inhibitors---NPPB, DIDS, and niflumic acid are classical inhibitors of Ca^{2+}-dependent Cl^- channel activity (20); they inhibit TMEM16A's channel activity with an IC_{50} of 10 μM for NPPB, 20 μM for DIDS, and 30 μM for niflumic acid (3,4). Recently, several other compounds were found to inhibit 16A's Cl^- channel activity (27,28). Tannic acid, EGCG, digallic acid, and $T16A_{inh}$-A01 inhibit 16A's Cl^- channel activity with IC_{50}'s of 6.4 μM, 100 μM, 3.6 μM, and 1.1 μM, respectively. To examine the effect of these inhibitors on TMEM16F's PS scramblase activity, *TMEM16F*$^{-/-}$ IFETs expressing TMEM16F were pre-treated with various concentrations of each compound for 5 min, treated with A23187 in the presence of the compound, and the PS exposure was monitored by FACS analysis. As shown in Fig. 8A, tannic acid and EGCG efficiently inhibited 16F's scramblase activity with IC_{50}'s of less than 1.0 μM, whereas NPPB, DIDS, digallic acid, and $T16A_{inh}$-A01 inhibited 16F's activity with IC_{50}'s of 80-300 μM. In particular, niflumic acid inhibited the scramblase only at high concentrations with an IC_{50} of more than 1000 μM. We then examined the effect of tannic acid, EGCG, digallic acid, and $T16A_{inh}$-A01 on the TMEM16A's Cl^- channel activity. That is, 293T cells were transfected with the expression

vector for TMEM16A, pre-treated for 5 min with each compound, and subjected to the patch-clamp analysis. In agreement with previous reports (27,28), the IC_{50} values of tannic acid, digallic acid, and $T16A_{inh}$-A01 for TMEM16A's Cl^- channel activity were less than 10 μM, while that of EGCG was higher than 100 μM (Fig. 8B). A plot of IC_{50} of TMEM16F *vs* TMEM16A (Fig. 8C) indicated that some chemicals ($T16A_{inh}$-A01 and digallic acid) efficiently inhibit TMEM16A's channel activity but not 16F's scramblase activity, while other compound (EGCG) inhibits the TMEM16F's activity more efficiently than 16A's activity.

DISCUSSION

The function of TMEM16F has so far been very controversial. Several groups including ours reported that TMEM16F has little or no Ca^{2+}-dependent Cl^- channel activity (7,10,29), while Yang *et al*. showed that it functions as a cation channel (11). On the other hand, other reports claimed that it works as Cl^- channel in dendritic cells (30), contributes to the outward rectifying Cl^- current for cell shrinkage during apoptosis (31), and functions as a volume-sensitive outwardly rectifying (VSOR) anion channel (32). Finally, Shimizu *et al*. (33) recently reported that TMEM16F functions as a Ca^{2+}-dependent Cl^- channel at high intracellular Ca^{2+} concentrations, but that it does not support VSOR currents activated by osmotic swelling or apoptotic stimulation. We found that a TMEM16F deficiency in human and mouse cells impairs Ca^{2+}-dependent phospholipid scrambling, and that its point mutation causes the constitutive scrambling of phospholipids on plasma membranes, leading us to conclude that TMEM16F is a phospholipid scramblase, or at least a subunit of such a scramblase (9,34). This PS-scrambling activity of TMEM16F was recently confirmed by Yang *et al.* (11) with mouse platelets and by Ehlen *et al.* (13) with developing bone cells.

Here, we confirmed that TMEM16F was required for Ca^{2+} ionophore-induced PS exposure in a mouse fetal thymocyte line. The defective PS-exposure in *TMEM16F*$^{-/-}$ cells could not be rescued by TMEM16A. In contrast, TMEM16A, but not 16F, carries a strong Ca^{2+}-dependent Cl^- channel activity in human 293T cells. Although we cannot formally rule out the possibility that TMEM16F has a Cl^- channel activity in IFETs, these results suggest that TMEM16F does not require Cl^- channel activity for its phospholipid scramblase activity, and that TMEM16A and 16F carry out distinct functions, Cl^- channel activity and phospholipid scramblase activity, respectively.

The N-terminal deletion and swapping in TMEM16A and 16F indicated that a 200-250 amino acid N-terminal domain that is necessary for TMEM16A's Cl^- channel and 16F's lipid scramblase activity is exchangeable between TMEM16A and 16F. Both TMEM16A and 16F are localized at plasma membranes. The N-terminal deletion of TMEM16A and 16F impaired their localization to the plasma membranes, and the deleted mutants stayed in the cytoplasm, likely in endoplasmic reticulum. In fact, a well-conserved signal for the protein export from endoplasmic reticulum (dibasic motif, [RK](x)[RK])

(35) was found in the N-terminal domain of TMEM16A and 16F (Fig. S1). An unexpected inability of nAF1 and nAF2 chimeras to be localized at plasma membranes suggested that the dibasic motif for the ER export alone is not sufficient for transporting proteins to plasma membranes. In deed, some proteins require multiple ER exit signals for efficient transport (36).

One of the common features of TMEM16A and 16F is the Ca^{2+} requirement for their activities, and an Arg-to-Leu point mutation at amino acid position 211 in mouse TMEM16F sensitizes it for Ca^{2+} (J.S. and S.N., unpublished result). It is therefore possible that the N-terminal domain of each protein is responsible for the Ca^{2+} responsiveness as well. Although we cannot find an EF hand motif for Ca^{2+} binding, a conserved putative calmodulin-binding site ([FILVW]xxx[FAILVW]xx[FAILVW]xxxxx[FILVW]) (37) exists in the N-terminal domain of TMEM16A and 16F (Fig. S1). Mutational analysis of this calmodulin-binding site, as well as other well-conserved motifs (GLYFxDGxRKVDYILVY and SLFFxDGxRRIDFILVY) with unknown function (Fig. S1), will be necessary to understand the function of the N-terminal region. A domain in the C-terminal region of TMEM16A and 16F was required for their stable protein expression, and was also exchangeable between the two proteins. Protein sumoylation is known to stabilize proteins (38,39). A putative sumolylation site ([VILMFPC]KxE or [ED]xK[LVIFP]) can be found in this region of TMEM16A and 16F (Fig. S1). Whether these motifs contributes to the stability of TMEM16A and 16F remains to be studied.

P4-type ATPase catalyzes phospholipid transport in an ATP-dependent manner and is a member of the P-type ATPases, which pump small cations and metal ions (40). In P4-type ATPase, the anionic residues that typically inhabit the ligand-binding pocket in cation pumps are replaced by a mixture of hydrophobic and polar uncharged residues, indicating that the same region may be involved in lipid transport (41). Similarly, since positively charged amino acids in the reentrance loop located between the 5^{th} and 6^{th} transmembrane regions in TMEM16A are essential for its ion permeability, Yang *et al*. (5) proposed that this domain works as a pore and filter for Cl^- ions. However, swapping this region between TMEM16A and 16F inactivated channel and scramblase activity (T.S., J.S., and S.N., unpublished results). We showed here that the residues conserved between TMEM16A and 16F in the "pore" region are required for the 16A's Cl^- channel activity and 16F's phospholipid scrambling activity. How the similar "pocket" in TMEM16A and 16F can act on both small ions and bulky phospholipids is not clear, and will be a challenging topic for future research.

The excessive extracellular transport of Cl^- ions appears to cause hypertension, diarrhea, cancer, and asthma, while its deficiency causes salivary gland dysfunction, cystic fibrosis, dry eye syndrome, intestinal hypomotility, and other diseases (20). TMEM16A, therefore, has been focused on as a drug target, and small molecules that function as its inhibitors or activators have been developed (27,28,42). However, since TMEM16F is involved in

the PS exposure of activated platelets and its defect causes bleeding disorders, inhibitors or activators of TMEM16A should be specific for TMEM16A. We here showed that among 7 different compounds (NPPB, DIDS, niflumic acid, tannic acid, EGCG, digallic acid and $T16A_{inh}$-A01) that inhibit TMEM16A's Cl^- channel activity (3,4,27,28), tannic acid and EGCG efficiently inhibited TMEM16F's scramblase activity, while the inhibitory activity of other compounds against TMEM16F was weak. These results suggest that the active sites of TMEM16A and 16F significantly differ, and agree with previous observations that tannic acid and EGCG have anti-thrombotic activities (43). The assignment of the binding sites for these compounds in TMEM16A and 16F will be useful for understanding how TMEM16A and 16F work as a Cl^- channel and phospholipid scramblase. Our results also indicate that more careful characterization of TMEM16 family members is necessary to develop better, more specific drugs.

REFERENCES

1. Hartzell, H. C., Yu, K., Xiao, Q., Chien, L. T., and Qu, Z. (2009) Anoctamin/TMEM16 family members are Ca^{2+}-activated Cl^- channels. *J. Physiol.* **587**, 2127-2139
2. Flores, C. A., Cid, L. P., Sepúlveda, F. V., and Niemeyer, M. I. (2009) TMEM16 proteins: the long awaited calcium-activated chloride channels? *Brazilian J. Med. Biol. Res.* **42**, 993-1001
3. Caputo, A., Caci, E., Ferrera, L., Pedemonte, N., Barsanti, C., Sondo, E., Pfeffer, U., Ravazzolo, R., Zegarra-Moran, O., and Galietta, L. (2008) TMEM16A, a membrane protein associated with calcium-dependent chloride channel activity. *Science* **322**, 590-594
4. Schroeder, B., Cheng, T., Jan, Y., and Jan, L. (2008) Expression cloning of TMEM16A as a calcium-activated chloride channel subunit. *Cell* **134**, 1019-1029
5. Yang, Y., Cho, H., Koo, J., Tak, M., Cho, Y., Shim, W., Park, S., Lee, J., Lee, B., Kim, B., Raouf, R., Shin, Y., and Oh, U. (2008) TMEM16A confers receptor-activated calcium-dependent chloride conductance. *Nature* **455**, 1210-1215
6. Duran, C., and Hartzell, H. C. (2011) Physiological roles and diseases of tmem16/anoctamin proteins: are they all chloride channels? *Acta Pharm. Sinic* **32**, 685-692
7. Schreiber, R., Uliyakina, I., Kongsuphol, P., Warth, R., Mirza, M., Martins, J., and Kunzelmann, K. (2010) Expression and function of epithelial anoctamins. *J. Biol. Chem.* **285**, 7838-7845
8. Huang, F., Rock, J. R., Harfe, B. D., Cheng, T., Huang, X., Jan, Y. N., and Jan, L. Y. (2009) Studies on expression and function of the TMEM16A calcium-activated chloride channel. *Proc. Nat. Acad. Sci. USA* **106**, 21413-21418
9. Suzuki, J., Umeda, M., Sims, P. J., and Nagata, S. (2010) Calcium-dependent phospholipid

scrambling by TMEM16F. *Nature* **468**, 834-838

10. Suzuki, J., Fujii, T., Imao, T., Ishihara, K., Kuba, H., and Nagata, S. (2013) Calcium-dependent Phospholipid Scramblase Activity of TMEM16 Protein Family Members. *J. Biol. Chem.* **288**, 13305-13316
11. Yang, H., Kim, A., David, T., Palmer, D., Jin, T., Tien, J., Huang, F., Cheng, T., Coughlin, S. R., Jan, Y. N., and Jan, L. Y. (2012) TMEM16F forms a Ca^{2+}-activated cation channel required for lipid scrambling in platelets during blood coagulation. *Cell* **151**, 111-122
12. Lhermusier, T., Chap, H., and Payrastre, B. (2011) Platelet membrane phospholipid asymmetry: from the characterization of a scramblase activity to the identification of an essential protein mutated in Scott syndrome. *J. Thromb. Haemost.* **9**, 1883-1891
13. Ehlen, H. W., Chinenkova, M., Moser, M., Munter, H. M., Krause, Y., Gross, S., Brachvogel, B., Wuelling, M., Kornak, U., and Vortkamp, A. (2013) Inactivation of Anoctamin-6/Tmem16f, a regulator of phosphatidylserine scrambling in osteoblasts, leads to decreased mineral deposition in skeletal tissues. *J. Bone Miner. Res.* **28**, 246-259
14. Charlesworth, G., Plagnol, V., Holmström, K. M., Bras, J., Sheerin, U.-M., Preza, E., Rubio-Agusti, I., Ryten, M., Schneider, S. A., Stamelou, M., Trabzuni, D., Abramov, A. Y., Bhatia, K. P., and Wood, N. W. (2012) Mutations in ANO3 cause dominant craniocervical dystonia: ion channel implicated in pathogenesis. *Am. J. Hum. Genet.* **91**, 1041-1050
15. Mizuta, K., Tsutsumi, S., Inoue, H., Sakamoto, Y., Miyatake, K., Miyawaki, K., Noji, S., Kamata, N., and Itakura, M. (2007) Molecular characterization of GDD1/TMEM16E, the gene product responsible for autosomal dominant gnathodiaphyseal dysplasia. *Biochem. Biophys. Res. Commun.* **357**, 126-132
16. Tsutsumi, S., Kamata, N., Vokes, T., Maruoka, Y., Nakakuki, K., Enomoto, S., Omura, K., Amagasa, T., Nagayama, M., Saito-Ohara, F., Inazawa, J., Moritani, M., Yamaoka, T., Inoue, H., and Itakura, M. (2004) The novel gene encoding a putative transmembrane protein is mutated in gnathodiaphyseal dysplasia (GDD). *Am. J. Hum. Genet.* **74**, 1255-1261
17. Vermeer, S., Hoischen, A., Meijer, R. P. P., Gilissen, C., Neveling, K., Wieskamp, N., de Brouwer, A., Koenig, M., Anheim, M., Assoum, M., Drouot, N., Todorovic, S., Milic-Rasic, V., Lochmüller, H., Stevanin, G., Goizet, C., David, A., Durr, A., Brice, A., Kremer, B., Warrenburg, B. P. C. v. d., Schijvenaars, M. M. V. A. P., Heister, A., Kwint, M., Arts, P., van der Wijst, J., Veltman, J., Kamsteeg, E.-J., Scheffer, H., and Knoers, N. (2010) Targeted next-generation sequencing of a 12.5 Mb homozygous region reveals ANO10 mutations in patients with autosomal-recessive cerebellar ataxia. *Am. J. Hum. Genet.* **87**, 813-819

18. Kashyap, M. K., Marimuthu, A., Kishore, C. J. H., Peri, S., Keerthikumar, S., Prasad, T. S. K., Mahmood, R., Rao, S., Ranganathan, P., Sanjeeviah, R. C., Vijayakumar, M., Kumar, K. V. V., Montgomery, E. A., Kumar, R. V., and Pandey, A. (2009) Genomewide mRNA profiling of esophageal squamous cell carcinoma for identification of cancer biomarkers. *Cancer Biol. Ther.* **8**, 36-46

19. Das, S., Hahn, Y., Nagata, S., Willingham, M., Bera, T., Lee, B., and Pastan, I. (2007) NGEP, a prostate-specific plasma membrane protein that promotes the association of LNCaP cells. *Cancer Res.* **67**, 1594-1601

20. Verkman, A. S., and Galietta, L. J. V. (2009) Chloride channels as drug targets. *Nat. Rev. Drug Discov.* **8**, 153-171

21. Morita, S., Kojima, T., and Kitamura, T. (2000) Plat-E: an efficient and stable system for transient packaging of retroviruses. *Gene Ther.* **7**, 1063-1066

22. Murai, K., Murakami, H., and Nagata, S. (1998) Myeloid-specific transcriptional activation by murine myeloid zinc finger protein-2. *Proc. Natl. Acad. Sci. USA* **95**, 3461-3466

23. Kuba, H., Yamada, R., and Ohmori, H. (2003) Evaluation of the limiting acuity of coincidence detection in nucleus laminaris of the chicken. *J. Physiol.* **552**, 611-620

24. Sheridan, J. T., Worthington, E. N., Yu, K., Gabriel, S. E., Hartzell, H. C., and Tarran, R. (2011) Characterization of the oligomeric structure of the $Ca^{(2+)}$-activated Cl^- channel Ano1/TMEM16A. *J. Biol. Chem.* **286**, 1381-1388

25. Ferrera, L., Caputo, A., Ubby, I., Bussani, E., Zegarra-Moran, O., Ravazzolo, R., Pagani, F., and Galietta, L. (2009) Regulation of TMEM16A chloride channel properties by alternative splicing. *J. Biol. Chem.* **284**, 33360-33368

26. Traut, T. W. (1988) Do exons code for structural or functional units in proteins? *Proc. Nat. Acad. Sci. USA* **85**, 2944-2948

27. Namkung, W., Phuan, P.-W., and Verkman, A. S. (2011) TMEM16A inhibitors reveal TMEM16A as a minor component of Calcium-activated Chloride channel conductance in airway and intestinal epithelial cells. *J. Biol. Chem.* **286**, 2365–2374

28. Namkung, W., Thiagarajah, J. R., Phuan, P. W., and Verkman, A. S. (2010) Inhibition of Ca^{2+}-activated Cl^- channels by gallotannins as a possible molecular basis for health benefits of red wine and green tea. *FASEB J.* **24**, 4178-4186

29. Duran, C., Qu, Z., Osunkoya, A. O., Cui, Y., and Hartzell, H. C. (2012) ANOs 3-7 in the anoctamin/Tmem16 Cl^- channel family are intracellular proteins. *Am. J. Physiol. Cell Physiol.* **302**, C482-493

30. Szteyn, K., Schmid, E., Nurbaeva, M. K., Yang, W., Münzer, P., Kunzelmann, K., Lang, F., and

Shumilina, E. (2012) Expression and functional significance of the Ca-activated Cl(-) channel ANO6 in dendritic cells. *Cell Physiol. Biochem.* **30**, 1319-1332

31. Martins, J. R., Faria, D., Kongsuphol, P., Reisch, B., Schreiber, R., and Kunzelmann, K. (2011) Anoctamin 6 is an essential component of the outwardly rectifying chloride channel. *Proc. Natl. Acad. Sci. USA* **108**, 18168-18172
32. Almaça, J., Tian, Y., Aldehni, F., Ousingsawat, J., Kongsuphol, P., Rock, J. R., Harfe, B. D., Schreiber, R., and Kunzelmann, K. (2009) TMEM16 proteins produce volume-regulated chloride currents that are reduced in mice lacking TMEM16A. *J. Biol. Chem.* **284**, 28571-28578
33. Shimizu, T., Iehara, T., Sato, K., Fujii, T., Sakai, H., and Okada, Y. (2013) TMEM16F is a component of a Ca^{2+}-activated Cl^- channel but not a volume-sensitive outwardly rectifying Cl^- channel. *Am. J. Physiol. Cell Physiol.* **304**, C748-759
34. Segawa, K., Suzuki, J., and Nagata, S. (2011) Constitutive exposure of phosphatidylserine on viable cells. *Proc. Natl. Acad. Sci. USA* **108**, 19246-19251
35. Giraudo, C. G., and Maccioni, H. J. F. (2003) Endoplasmic reticulum export of glycosyltransferases depends on interaction of a cytoplasmic dibasic motif with Sar1. *Mol. Biol. Cell.* **14**, 3753-3766
36. Barlowe, C. (2003) Signals for COPII-dependent export from the ER: what's the ticket out? *Trends Cell Biol.* **13**, 295-300
37. Rhoads, A. R., and Friedberg, F. (1997) Sequence motifs for calmodulin recognition. *FASEB J.* **11**, 331-340
38. Johnson, E. S. (2004) Protein modification by SUMO. *Annu. Rev. Biochem.* **73**, 355-382
39. Klenk, C., Humrich, J., Quitterer, U., and Lohse, M. J. (2006) SUMO-1 Controls the Protein Stability and the Biological Function of Phosducin. *J. Biol. Chem.* **281**, 8357–8364
40. Folmer, D., Elferink, R., and Paulusma, C. (2009) P4 ATPases - lipid flippases and their role in disease. *Biochim. Biophys. Acta* **1791**, 628-635
41. Muthusamy, B.-P., Natarajan, P., Zhou, X., and Graham, T. R. (2009) Linking phospholipid flippases to vesicle-mediated protein transport. *Biochim. Biophys. Acta* **1791**, 612-619
42. Namkung, W., Yao, Z., Finkbeiner, W. E., and Verkman, A. S. (2011) Small-molecule activators of TMEM16A, a calcium-activated chloride channel, stimulate epithelial chloride secretion and intestinal contraction. *FASEB J.* **25**, 4048-4062
43. Kang, W.-S., Lim, I.-H., Yuk, D.-Y., Chung, K.-H., Park, J.-B., Yoo, H.-S., and Yun, Y.-P. (1999) Antithrombotic Activities of Green Tea Catechins and (–)-Epigallocatechin Gallate. *Thromb. Res.* **96**, 229-237

Acknowledgments---We are grateful to H. Ohmori (Department of Physiology, Graduate School of Medicine, Kyoto University) for valuable advice on electrophysiology. We thank M. Fujii for secretarial assistance.

FOOTNOTES

*This work was supported in part by Grants-in-Aid from the Ministry of Education, Science, Sports, and Culture in Japan.

[1]To whom correspondence should be addressed: Shigekazu Nagata, Department of Medical Chemistry, Graduate School of Medicine, Kyoto University, Yoshida, Sakyo-ku, Kyoto 606-8501, Japan, Tel: 81-75-753-9441, Fax: 81-75-753-9446, E-mail: snagata@mfour.med.kyoto-u.ac.jp

[2]Abbreviations used are: IFET, immortalized fetal thymocyte; PS, phosphatidylserine; EGCG, epigallocatechin-3-gallate; $T16A_{inh}$-A01, 2-(5-ethyl-4-hydroxy-6-methylpyrimidin-2-ylthio)-N-(4-(4-methoxyphenyl) thiazol-2-yl)acetamide; NPPB, 5-nitro-2-(3-phenylpropylamino)benzoic acid; DIDS, 4,4'-diisothiocyanostilbene-2,2'- disulfonic acid; niflumic acid, 2-[3-(trifluoromethyl)anilino] nicotinic acid; DSP, dithiobis[succinimidylpropionate];

FIGURE LEGENDS

FIGURE 1. **Distinct functions of TMEM16A and TMEM16F.** (*A*) Ca^{2+}-dependent Cl^- channel activity. HEK293T cells were co-transfected with the empty vector (-) or an expression vector for TMEM16A or TMEM16F, together with pMAX-GFP. At left, the expression levels of TMEM16A and 16F were analyzed by western blotting with an anti-Flag mAb 48 h after the transfection. At right, membrane currents at the indicated voltage pulses (mV) of GFP-positive cells were measured by whole-cell patch clamp analysis. Experiments were done 3-5 times, and the average values are plotted with S.D. (bars) (top). In the lower panel, the outward rectification of the Cl^- current was traced at -120 to +120 mV in 10-mV steps. (*B*) Ca^{2+}-dependent PS scrambling activity. *TMEM16F*$^{-/-}$ IFETs were stably transformed by the empty retroviral vector (-), or vector for the Flag-tagged TMEM16A (16A) or TMEM16F (16F). At left, the transformants were analyzed by western blotting with an anti-Flag mAb. At right, the cells were treated with 3 μM A23187. Their ability to bind Cy5-labeled Annexin V was followed by flow cytometry, and expressed in mean fluorescence intensity (*MFI*).

FIGURE 2. **Dimeric structure of TMEM16A and 16F.** HEK293T cells that had been transfected with the expression vector for Flag-tagged TMEM16A (*A*) or TMEM16F (*B*), and *TMEM16F*$^{-/-}$ IFET transformants expressing the Flag-tagged TMEM16A (*A*) or TMEM16F (*B*) were treated with the indicated concentrations of DSP, washed, and lysed in RIPA buffer. The lysates were separated by 5% SDS-PAGE, and analyzed by western blotting with an anti-Flag mAb.

FIGURE 3. **N-terminal deletion of TMEM16A and 16F.** (*A-D*) Effect of N-terminal deletion on TMEM16A's

Cl^- channel activity. (*A*) N-terminal deletion mutants of TMEM16A are shown schematically. Numbers in the top column and at the bottom indicate the exon number, and the amino acid position where the deletion mutants start, respectively. TM1, 1st transmembrane region. The mutants that showed Cl^- channel activity are marked by ○, and the mutants that did not are by ×. (*B*) Membrane currents at the indicated voltage pulses (mV) were measured by whole-cell patch clamp analysis of 293T cells transfected with the expression vector for the deletion mutant (Δexon 1, Δexon 1-2, Δexon 1-5, or Δexon 1-7 of TMEM16A). (*C*) 293T cells that had been transfected with the expression vector for TMEM16A or its N-terminal deletion mutants were separated by 5-10 % SDS-PAGE, and analyzed by western blotting with an anti-Flag mAb. (*D*) HEK293T cells were transfected with the expression vectors for GFP-tagged wild-type or deletion mutants (Δ1 and Δ1-2) of TMEM16A, and observed by confocal microscope. (*E-H*) Effect of N-terminal deletion on TMEM16F's phospholipid scramblase activity. (*E*) N-terminal deletion mutants of TMEM16F are shown. Numbers in the top column and at the bottom indicate the exon number and the amino acid position where the deletion mutants start, respectively. The mutants that showed the scramblase activity are marked by ○, and the mutants that did not are by ×. (*F*) Cy5-Annexin V binding to the A23187-treated *TMEM16F*$^{-/-}$ IFET transformants expressing the full-length TMEM16F or its deletion mutant (Δexon 1, Δexon 1-2, Δexon 1-3, Δexon 1-4, Δexon 1-5, Δexon 1-6, or Δexon 1-7) was followed by FACSCalibur for 9 min, and expressed in MFI. (*G*) Western blotting of *TMEM16F*$^{-/-}$ IFET transformants expressing TMEM16F or its deletion mutants. Cell lysates were separated by 5-10 % SDS-PAGE, and analyzed with an anti-Flag mAb. (*H*) HEK293T cells were transfected with the expression vectors for GFP-tagged wild-type or deletion mutants (Δ1-2 and Δ1-3) of TMEM16F, and observed by confocal microscope.

FIGURE 4. **C-terminal deletion of TMEM16A and 16F.** (*A*) Effect of C-terminal deletion on the expression of TMEM16A. At upper panel, structure of the C-terminal deletion mutants of TMEM16A is schematically shown. Numbers in the top column indicate the exon number. TM6, TM7, and TM8 represent the 6th, 7th, and 8th transmembrane regions. Numbers at the bottom indicate the amino acid position where the deletion mutants end. In lower panel, the cell lysates from 293T cells that had been transfected with the vector for full-length TMEM16A (16A) or its C-terminal deletion mutants (Δexon 24, Δexon 23-24, Δexon 22-24, Δexon 21-24, and Δexon 20-24) were separated by 5-10% SDS-PAGE, and analyzed by western blotting with an anti-Flag mAb. As a control, western blotting was performed with an anti-α-tubulin mAb, and shown at the bottom. (*B*) Effect of C-terminal deletion on the expression of TMEM16F. Structure of the C-terminal deletion mutant of TMEM16F is shown. Numbers in the top column indicate the exon number. TM6, TM7, and TM8 represent the 6th, 7th, and 8th transmembrane regions. Numbers at the bottom indicate the amino acid position where the deletion mutant ends. In lower panel, the lysates from *TMEM16F*$^{-/-}$ IFET transformants expressing the full-length TMEM16F

(16F) or its C-terminal deletion mutant (Δexon 20) were separated by 5-10% SDS-PAGE, and analyzed by western blotting with an anti-Flag mAb. As a control, western blotting was performed with an anti-α-tubulin mAb, and the results are shown at the bottom.

FIGURE 5. **N-terminal chimeric mutants between TMEM16A and 16F.** (*A*) Structures of the two sets of N-terminal chimeric molecules (nFA and nAF series) are schematically shown. In each chimera, the regions in blue are from TMEM16A, and those in brown are from TMEM16F. Numbers in the columns indicate the exon number, and the position at which the chimeric molecule was prepared is indicated by a red bar with the construct number. The constructs with which Cl^--channel or phospholipid scramblase activity was detected are marked by ○, while those that did not show the channel or scramblase activity are marked by ×. (*B*) The expression levels of the chimeric proteins in 293T cells for the nFA series and in *TMEM16F*$^{-/-}$ IFETs for the nAF series were analyzed by western blotting with an anti-Flag mAb. (*C*) The Cl^- channel activity was measured by whole-cell patch clamp analysis of 293T cells transfected with the nFA series of chimeric constructs. (*D*) Cy5-Annexin V binding to A23187-treated *TMEM16F*$^{-/-}$ IFET transformants expressing empty vector (-), or TMEM16F (16F) or nAF series of chimeric constructs was followed for 9 min using FACSCalibur, and expressed in MFI. (*E*) HEK293T cells were transfected with the expression vectors for GFP-tagged nAF1, 2, or 3, and observed by confocal microscope.

FIGURE 6. **C-terminal chimeric mutants between TMEM16A and 16F.** (*A*) Structures of the two sets of C-terminal chimeric molecules (AFc and FAc series) are shown schematically. In each chimera, the regions in blue are from TMEM16A, and those in brown are from TMEM16F. Numbers in the column indicate the exon number, and the position at which the chimeric molecule was prepared is indicated by a red bar with the construct number. The constructs with which Cl^--channel or phospholipid scramblase activity was detected are marked by ○, while those that did not show the channel or scramblase activity are marked by ×. (*B*) The expression level of the chimeric proteins in 293T cells for the AFc series and in *TMEM16F*$^{-/-}$ IFETs for the FAc series was analyzed by western blotting with an anti-Flag mAb. (*C*) Membrane currents at the indicated voltage pulses (mV) were measured by whole-cell patch clamp analysis of 293T cells transfected with the AFc series of chimeric constructs. (*D*) Cy5-Annexin V binding to the A23187-treated *TMEM16F*$^{-/-}$ IFET transformants expressing empty vector (-), or full-length TMEM16F (16F) or the FAc series of chimeric constructs was followed for 9 min using FACSCalibur, and expressed in MFI.

FIGURE 7. **Point mutations in TMEM16A and 16F.** (*A*) The amino acid sequences of mouse TMEM16A (position from 599 to 702) and 16F (position from 574 to 671) were aligned to obtain maximum homology.

Amino acids identical between TMEM16A and 16F are orange, and the transmembrane regions are green. The numbers above and below the sequence indicate the amino acid positions in TMEM16A and 16F, respectively. Amino acids mutated to glutamic acid are in red. (*B*) Cell lysates of HEK293T cells that had been transfected with the expression vector for TMEM16A or its indicated mutants (left panel), or the cell lysates of *TMEM16F*$^{-/-}$ IFET transformants expressing TMEM16F or its indicated mutants (right panel) were analyzed by western blot with anti-Flag antibody. Left panel: lane 1, TMEM16A; lane 2, R617E mutant; lane 3, K641E mutant; lane 4, K664E mutant. Right panel: lane 1, TMEM16F; lane 2, R592E mutant; lane 3, K616E mutant; lane 4, R592E/K616E mutant; lane 5, K638E mutant. (*C*) Membrane currents at the indicated voltage pulses (mV) were measured by the whole-cell patch clamp analysis of 293T cells transfected with the expression vector for TMEM16A or its indicated point mutants. (*D*) Cy5-Annexin V binding to the A23187-treated *TMEM16F*$^{-/-}$ IFET transformants expressing empty vector (-), or TMEM16F (16F) or its indicated point mutants was followed for 9 min using FACSCalibur, and expressed in MFI.

FIGURE 8. **Effect of various compounds on the PS scramblase activity of TMEM16F and on the Cl^- channel activity of TMEM16A.** (*A*) *TMEM16F*$^{-/-}$ IFET transformants expressing TMEM16F were pre-treated for 5 min with the indicated concentrations of various Cl^- channel inhibitors (tannic acid, EGCG, digallic acid, $T16A_{inh}$-A01, NPPB, DIDS, or niflumic acid), followed by stimulation with A23187 and flow cytometry analysis with Cy5-labeled Annexin V. The mean fluorescence intensity observed at 5 min was determined, and the data are expressed as the percentage of fluorescent intensity detected without the compound. Experiments were carried out at least three times, and the average values are plotted with S.D. (bars). (*B*) 293T cells transfected with the expression vector for TMEM16A were incubated for 5 min with the indicated concentrations of tannic acid, EGCG, digallic acid, or $T16A_{inh}$-A01, and membrane currents at 120 mV were measured by whole-cell patch clamp analysis. The data are expressed as the percentage of Cl^- current detected without compound. Experiments were carried out at least three times, and the average values are plotted with S.D. (bars). (*C*) IC_{50} values of tannic acid, EGCG, digallic acid, and $T16A_{inh}$-A01 for TMEM16A (*x*-axis) and 16F (*y*-axis) were determined, and plotted.

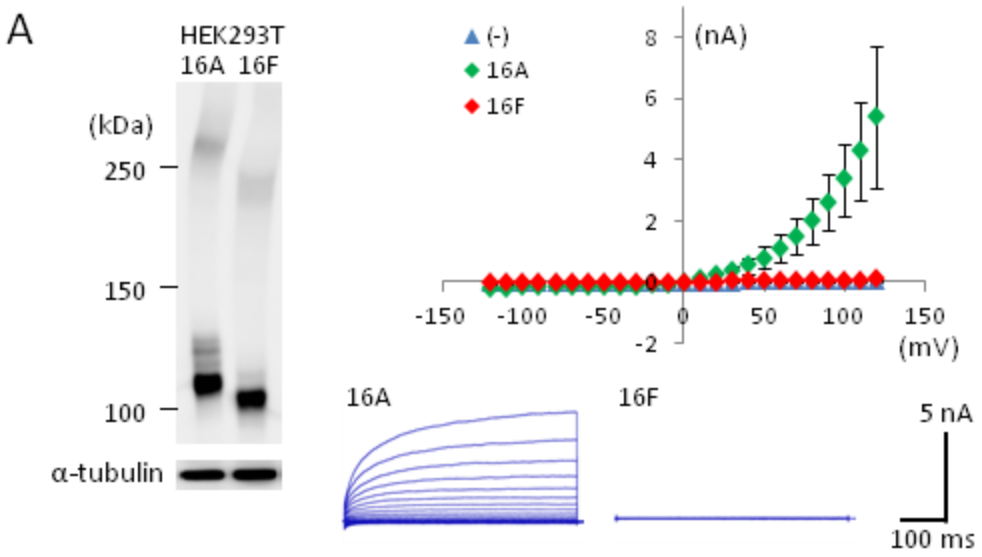

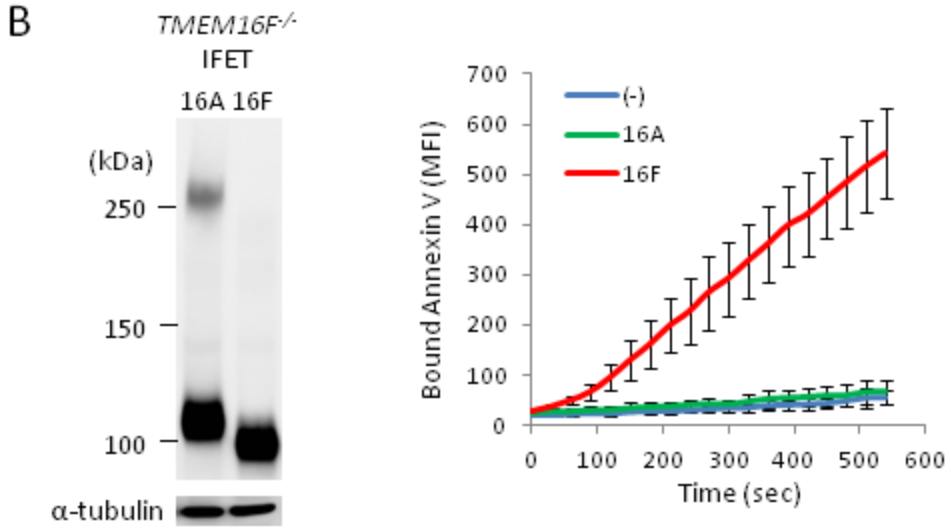

Suzuki et al. Figure 1

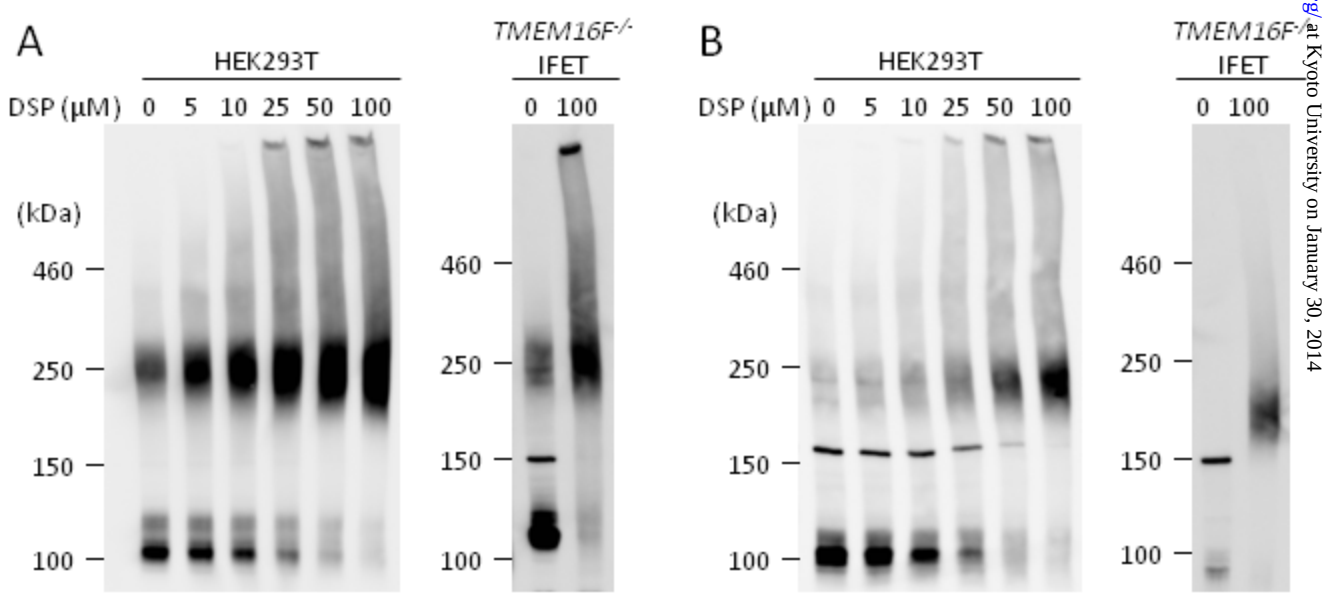

Suzuki et al. Figure 2

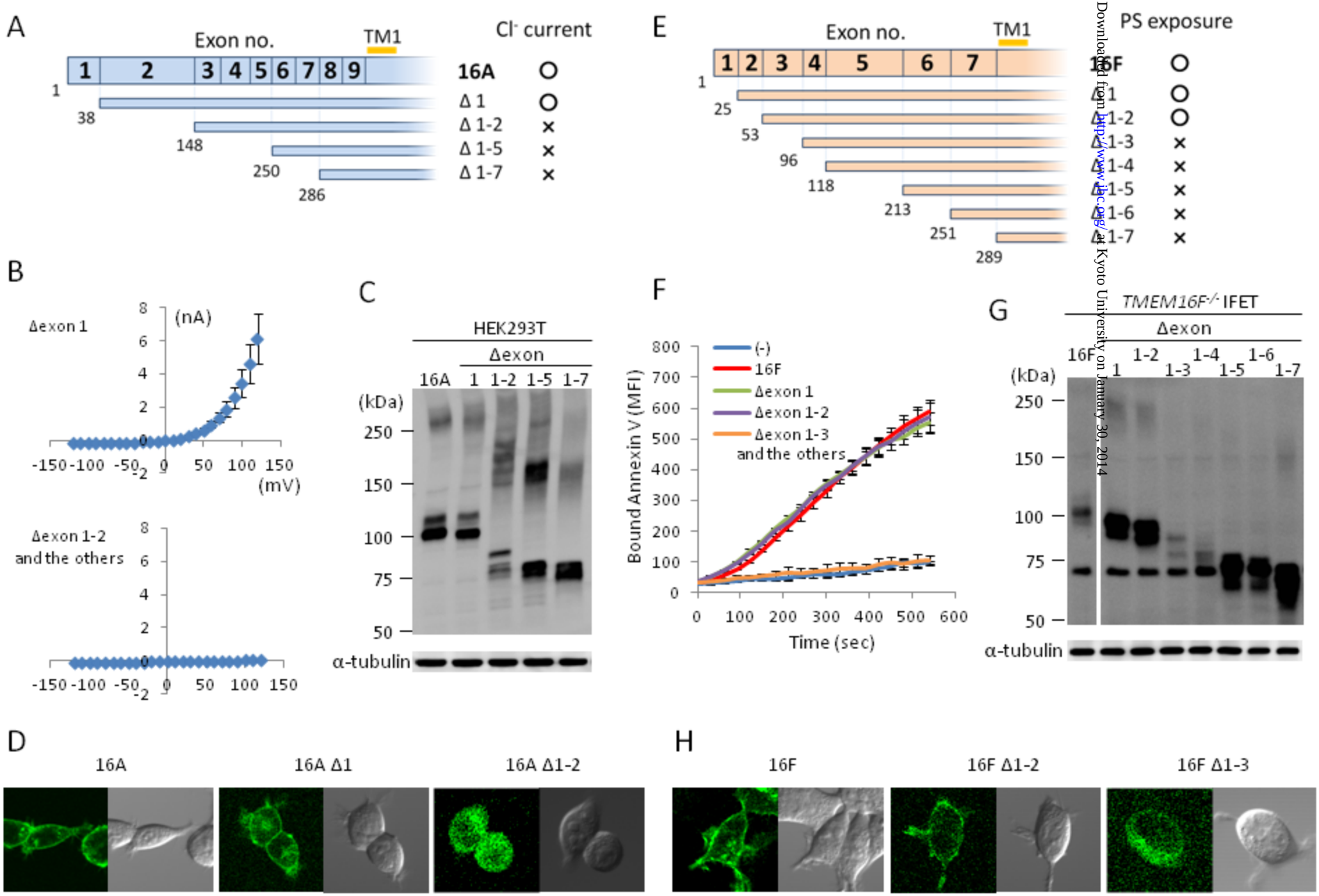

Suzuki et al. Figure 3

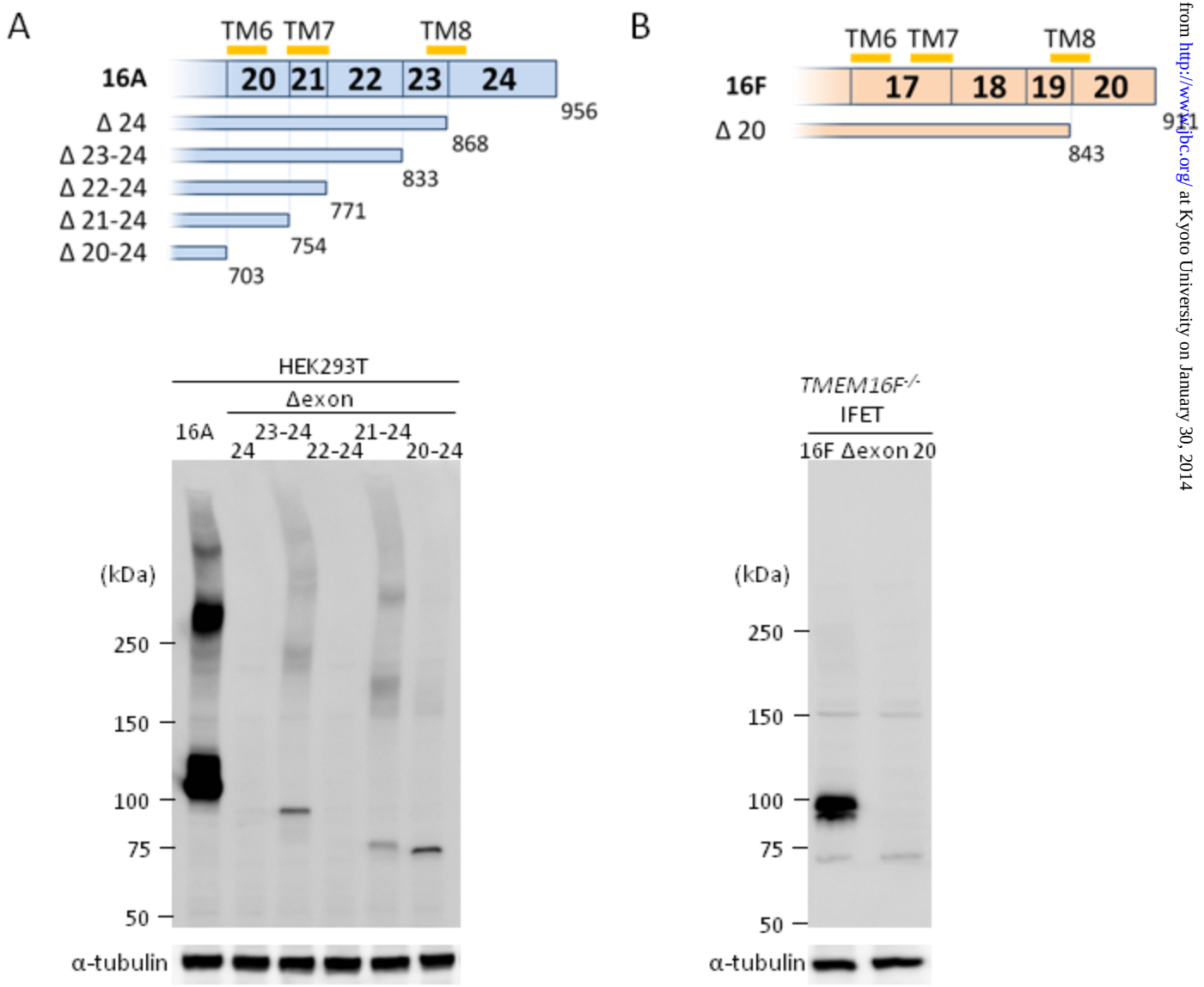

Suzuki et al. Figure 4

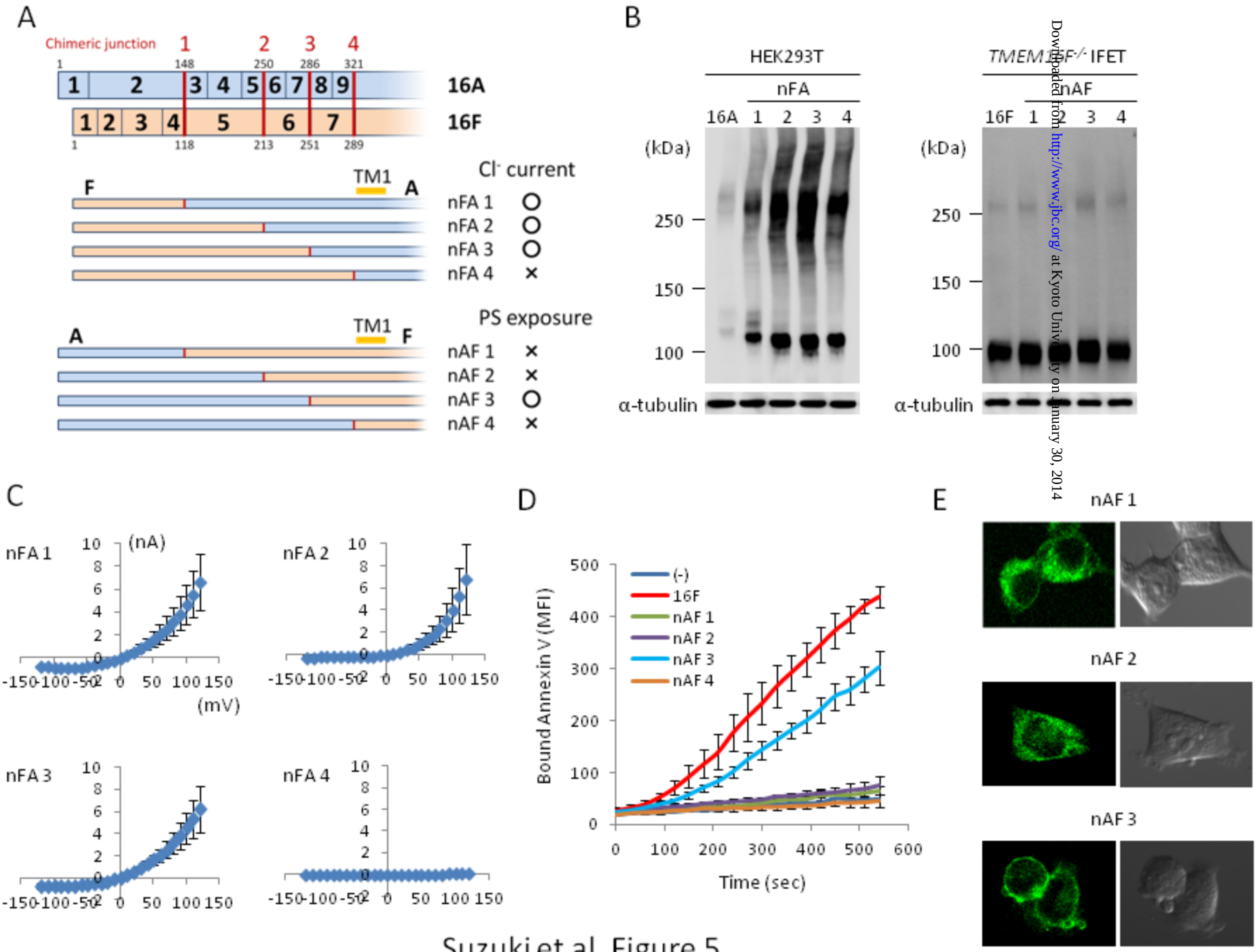

Suzuki et al. Figure 5

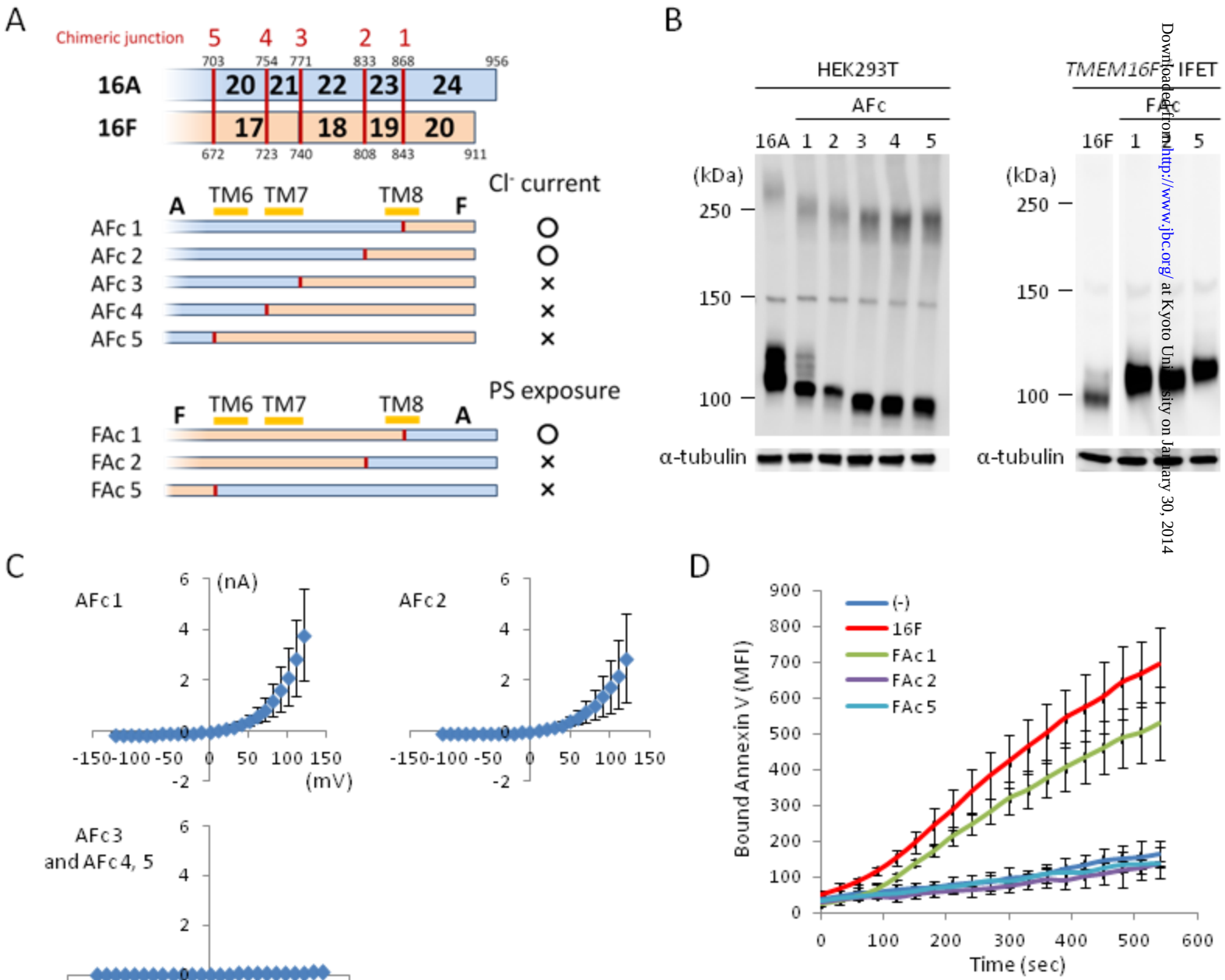

Suzuki et al. Figure 6

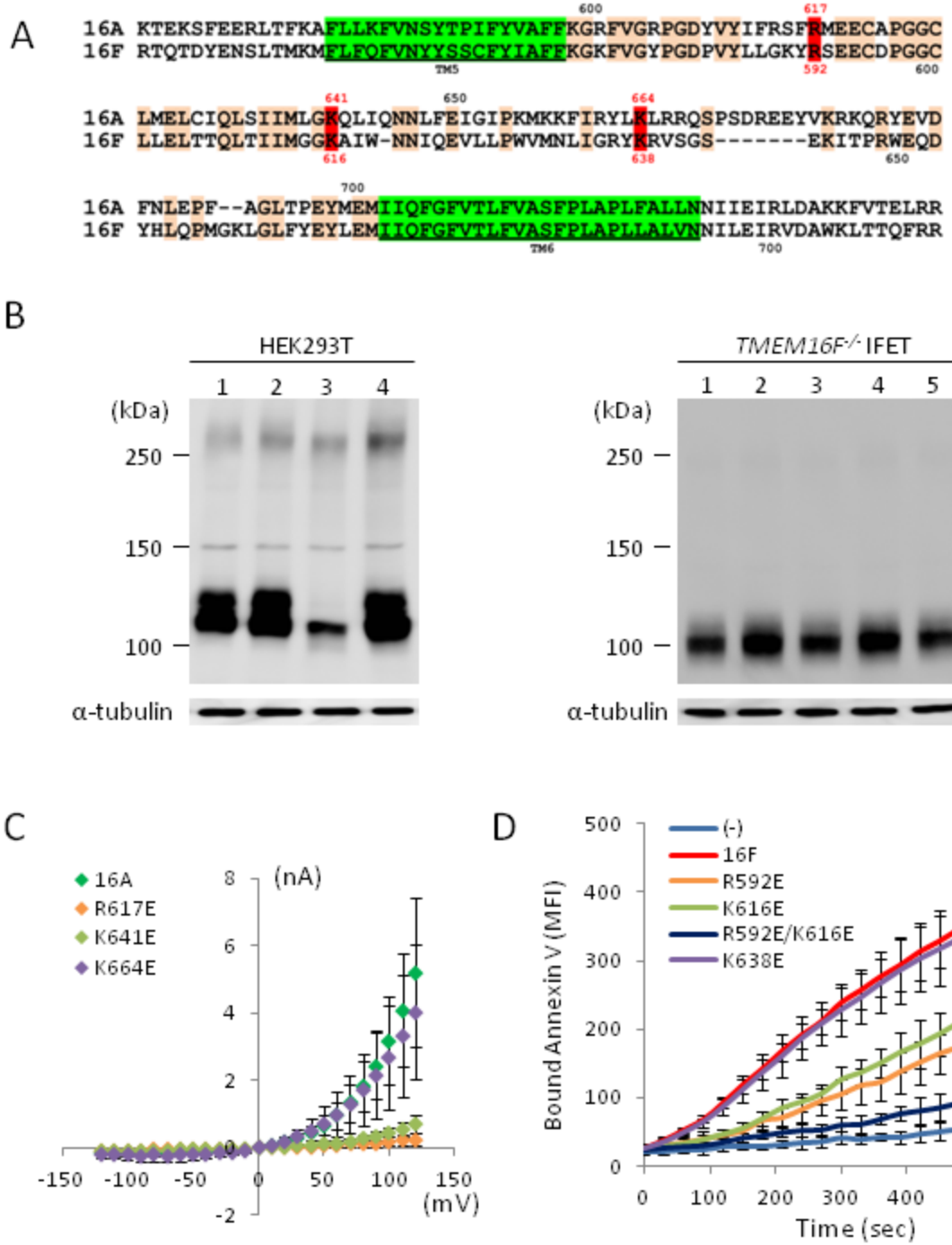

Suzuki et al. Figure 7

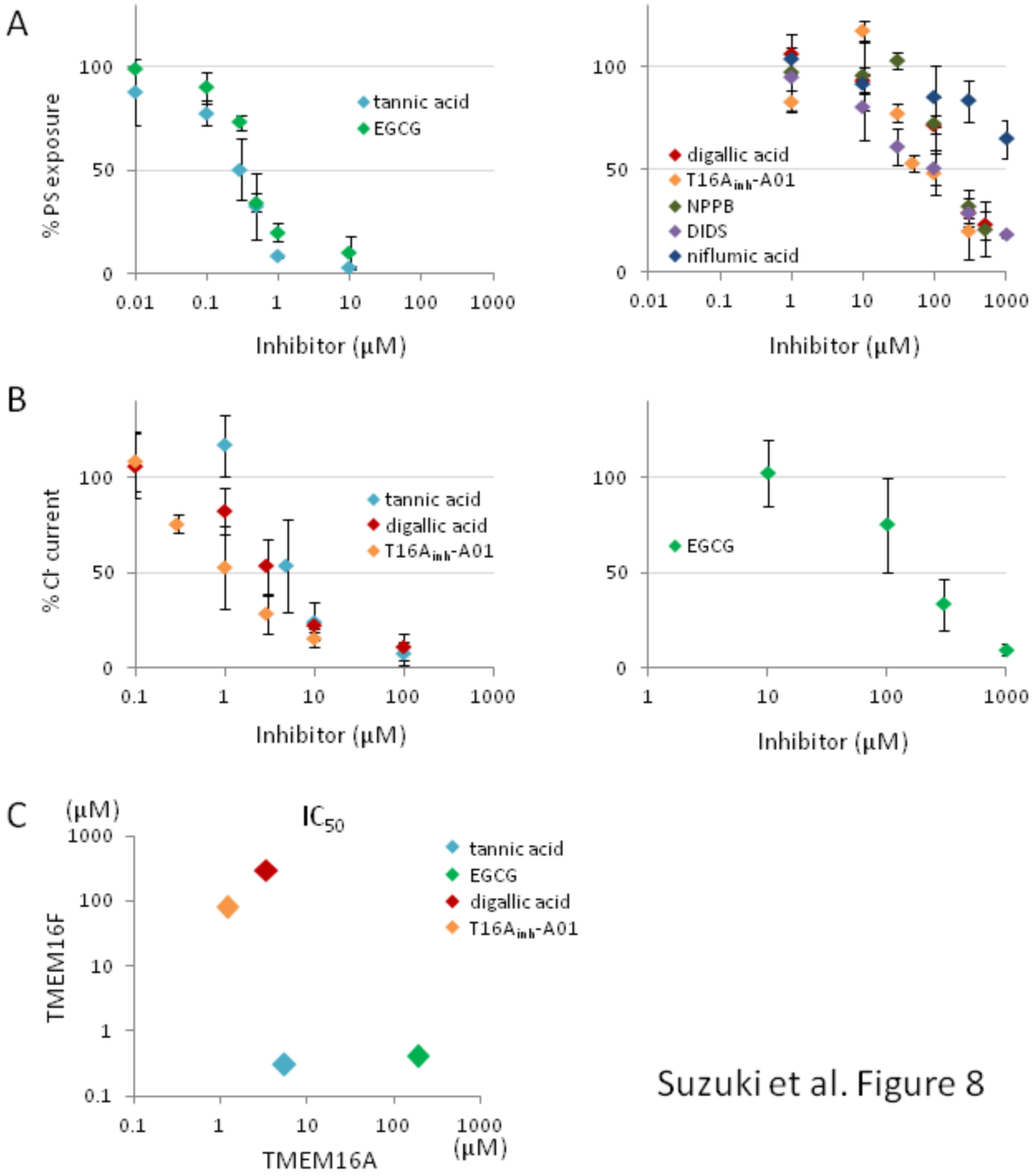

Suzuki et al. Figure 8